Available online at www.sciencedirect.com
SCIENCE DIRECT
Journal of Sound and Vibration 296 (2006) 583–601
JOURNAL OF SOUND AND VIBRATION
www.elsevier.com/locate/jsvi

Predictive model of squeal noise occurring on a laboratory brake

Oliviero Giannini*, Aldo Sestieri

Department of Mechanics and Aeronautics, University of Rome "la Sapienza", Italy

Received 14 December 2004; received in revised form 23 February 2006; accepted 23 February 2006
Available online 9 June 2006

Abstract

This paper on brake squeal instability presents a reduced order model of a laboratory brake considered in a previous paper, and presents a description of the squeal mechanism occurring during experiments.

The model uses the modal parameters of the laboratory brake components, the disc and the caliper, when they are not in contact between them. Successively, the caliper and the disc are put in contact through the pad that is modeled as a one degree of freedom system while the Coulomb law models the friction interaction between them. No stick slip motion of the pad is considered, because it was not observed in the experimental tests. As a result the model is linear and particularly suited for a parametric analysis.

The stability of the model is studied by a complex eigenvalue analysis and the obtained results show a good agreement with the experimental data, provided that the key parameters of the model are consistent with the experimental set-up. The key role of the disc and the pad dynamics are discussed.

1. Introduction

Brake squeal is a very complex phenomenon, involving different disciplines (e.g. vibrations, tribology, acoustics, etc.) so that many different approaches to the problem were considered in the past and many different explanations on squeal origin were proposed. So far, however, there is not yet a comprehensive understanding of the phenomenon.

The study presented in this paper provides a description of the squeal phenomenon, able to explain the behavior manifested by a laboratory brake.

The overall goal of this research is the identification of a path leading to the physical description of the interaction between friction and the dynamics of the system that destabilizes the brake. The simplification of the problem is the key of the method proposed.

In fact, it is generally accepted that one of the main difficulties encountered in studying brake squeal is the high complexity of the brake apparatus. Such complexity, together with the everpresence of data dispersion in experimental studies, is one of the main reasons that did not permit yet to have an efficient control of brake squeal.

*Corresponding author. Fax: +39 6 484854.
E-mail address: oliviero.giannini@uniroma1.it (O. Giannini).

0022-460X/$ - see front matter © 2006 Published by Elsevier Ltd.
doi:10.1016/j.jsv.2006.02.022

Nomenclature

h	width of the pad
J	moment of inertia of the pad
k_n	normal stiffness of the pad
k_p	in-plane stiffness of the pad
k_r	rotational stiffness of the pad
$\mathbf{K}$	coupling stiffness matrix
$\mathbf{K}^*$	stiffness matrix of the coupled system
$\mathbf{K}'$	stiffness matrix of the expanded system
$\mathbf{K}_0$	stiffness matrix of the uncoupled system
$\mathbf{K}_{d1}$, $\mathbf{K}_{d2}$	stiffness matrices of the uncoupled disc
l_c	distance between the center of mass of the pad and the contact point
m	mass of the pad
$\mathbf{M}_0$	mass matrix of the uncoupled system
$\mathbf{M}'$	mass matrix of the expanded system
(n,m)	mode uncoupled disc mode with n nodal circumferences and m nodal diameter
(n,m−)	mode coupled disc mode with a nodal diameter passing through the contact point
(n,m+)	mode coupled disc mode with an anti-nodal diameter passing through the contact point
N_b	number of uncoupled beam modes
N_{d1},N_{d2}	number of uncoupled disc modes
p	modal coordinates of the uncoupled disc
$P(x_0, y_0)$	contact point
q	modal coordinates of the uncoupled beam
SI_a	squeal index A
SI_b	squeal index B
z_d	bending displacement of the disc
z_b	bending displacement of the beam
α	misalignment angle between the plane of the disc and the axis of the beam
μ	friction coefficient
ϕ_i	ith mode of the uncoupled disc
ψ_i	ith mode of the uncoupled beam
Λ_b	stiffness matrix of the uncoupled beam
$\mathbf{\Lambda}_{d1}$, $\mathbf{\Lambda}_{d2}$	stiffness matrices of the uncoupled disc

Several models were developed in the past century on the squeal problem: in the early years, among the others, Mills [1] and Fosberry and Holubecki [2,3] tried to correlate the occurrence of squeal during experiments with a negative slope of the friction coefficient–relative velocity curve (μ–v_r), while Spurr [4] proposed a sprag-slip theory, followed later by Earles et al. [5,6] and Jarvis and Mills [7]. In 1972 North [8,9] published the first experimental work on a real brake apparatus and correlated his measurements with a model. In his work the friction was modeled as a follower force and a possible instability condition was met by using only a constant friction coefficient.

Many of such models use an analytical formulation for the brake rotor, considered as a flat, homogeneous annular plate, clamped on the internal radius: among the others, Mottershead [10], and Chan et al. [11], equate the squeal to two different set of instabilities: the first set produces instabilities at sub-critical parametric resonances; the second set, caused by the friction interaction between disc and pad, destabilizes the backwards waves of all the modes with nodal diameters. Ouyang et al. [12,13] found that an in-plane damper acting on the pad induces instability at additional parametric resonances, while it reduces the unstable regions in correspondence to other resonances.

Later models use a Finite Element formulation to describe the complex geometry of the brake and use the determined eigenvalues and eigenvectors to build a reduced order model of the system. Such models are generally more suitable for a parametric analysis as shown in Refs. [14,15] and, despite the computational time, the stability analysis can be performed directly on the FE model [16–18].

In this paper, to avoid the difficulties arising from the complexity of a real brake, a predictive model of squeal noise occurring in a simplified experimental rig, able to reproduce the main features of a commercial disc brake but with a more simple geometry, is proposed. This set-up, called "the laboratory brake", allows for a simplified modeling. The laboratory brake and the related experimental results are described in [19].

The proposal of using a simplified brake system to obtain reliable data during tests and a better understanding of the squeal mechanism is not original. In fact, in the past many research groups, Akay et al. [20], Tucinda et al. [15,21], Allgaier et al. [18,22], involved in the study of brake squeal phenomenon, conducted extensive analyses of the beam-on disc set-up.

The study of the squeal events with the beam-on-disc [20] allowed to model the friction interaction between a beam and a disc that leads to the unstable behavior. The developed models were able to predict the conditions necessary for the squeal event; however, such good results are not obtained when using the same methodology, applied to the analysis of a complex disc brake apparatus.

Thus, the authors considered that there was still the need for a simplified experimental set-up that can be considered as the ''trait d'union'' between the beam-on-disc and a commercial brake. This is the aim of the designed laboratory brake.

The predictive model presented in this paper is a reduced-order model of the laboratory brake. The dynamic model is built by using some data derived from the experimental set-up, e.g. the mass, the normal stiffness and the damping loss factor of the pad, and by an experimental modal analysis performed on the uncoupled components of the brake (disc and caliper that, in the considered set-up, is obtained by a couple of beams), and is able to predict the squeal conditions occurred during experiments.

The overall aim of this work is that of increasing step by step the complexity of the set-up and, accordingly, the complexity of the model up to a commercial brake system. At each step the model must be able to predict the squeal occurrence and, at each step, the model must be improved to account for other aspects of the brake-pad-caliper interaction. This paper presents the first part of the work.

2. Description of the model

The laboratory brake is an experimental rig designed to be, on one hand, a reliable set-up, able to produce squeal in a controlled and reproducible way and, on the other hand, to be as close as possible to a commercial brake.

The experimental set-up consists of a disc constrained on a rotating shaft, a pair of beams that represent the caliper, and two small brake pads that connect the disc and the beams (Fig. 1).

With respect to the beam on disc set-up [20], the laboratory brake is characterized by two major improvements:

- the coupling between the out-of-plane vibrations of the disc and its in-plane motion is far less strong and much closer to a real brake. In fact, in the beam on disc the angle between the beam and the disc is close to 45°. This allows the friction force to excite easily the bending vibrations of the beam and these vibrations have a consistent component in the out-of-plane direction. The laboratory brake has two beams (representing the caliper) almost parallel to the disc plane and, thus, a geometry much closer to a real brake, characterized by a weak coupling between in and out-of-plane vibrations;
- the beam on disc is characterized by two low-damped structures interacting through the friction force. In the laboratory brake, on the contrary, the brake pads are characterized by a high damping loss factor (the measurements provide a 6% value) that change consistently the modal interaction leading to instability.

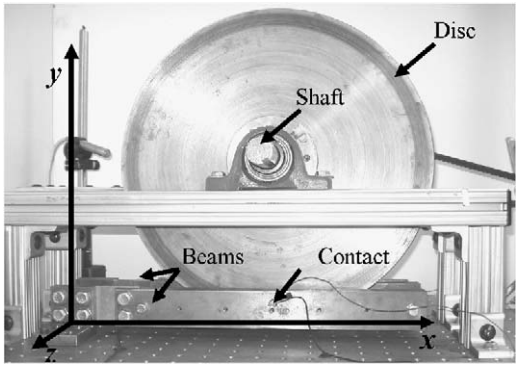

Fig. 1. Experimental set-up.

Therefore, the new developed set-up represents a significant improvement of the beam on disc, permitting to understand better the squeal emission, accounting for mechanisms that cannot be obtained by previous set-ups.

The experimental study performed with the laboratory brake [19] provides important guide-lines for building an adeguate model of the squeal behavior occurring in this set-up:

- first of all, since the squeal frequencies depend on the out-of-plane dynamics of the system, the transverse modes of the disc and the beams within the range of interest must be included in the model;
- moreover, double modes of the disc must be included in the model (the disc is symmetric when uncoupled to the rest of the system) and the split between them, arising when the disc is connected to the beams through the pads, must be consistent with the experimental results;
- finally, considering that the experimental tests show no stick-slip condition during instabilities, it is possible to assume that the relative velocity between disc and pads does not change its direction, and it is possible to model the friction between disc and pads by the Coulomb's law with constant μ.

Such considerations lead to a linear description of the interaction between disc and pads that, together with a reduced number of degrees of freedom, allows for a fast yet straightforward analysis of the behavior of the model and, through a complex eigenvalue analysis, to the determination of instability conditions.

The model starts from the modal description of the disc and the two beams, when they are not in contact. During the tests, the transverse vibrations of the disc and the two beams are excited at a point coincident with the contact point. The FRF at the drive point is processed by the ICATS[1] software to obtain the modal parameters. Specifically, from the measurement performed in uncoupled conditions, the stiffness and mass matrices of the laboratory brake component are retrieved.

There are two stiffness and mass modal matrices $\mathbf{K}_{d1}$ and $\mathbf{K}_{d2}$ of the disc because of the double modes of the disc[2]: the first set is derived from the modes that have an antinode in the contact position, the second from the modes that have a node. All the stiffness values are complex to account for the hysteretic damping of the brake components. The stiffness and mass matrices are:

- the modal stiffness matrices $\mathbf{K}_{d1}$ and $\mathbf{K}_{d2}$ of the disc;
- the modal mass matrices $\mathbf{M}_{d1}$ and $\mathbf{M}_{d2}$ of the disc;
- the modal stiffness matrix $\mathbf{K}_b$ of the beams;
- the modal mass matrix $\mathbf{M}_b$ of the beams.

Since the eigenvectors are normalized to unit modal mass, the matrices $\mathbf{M}_{d1}$, $\mathbf{M}_{d2}$, and $\mathbf{M}_b$ (from now on denoted by $\mathbf{I}$) are identity matrices and the matrices $\mathbf{K}_{d1}$ $\mathbf{K}_{d2}$ $\boldsymbol{K}_b$ are diagonal and represent the eigenvalues of the uncoupled system (from now on denoted by $\mathbf{\Lambda}$).

When assembling together the whole system, each mode of the structure, considered as a single degree of freedom system, is coupled with the vibration of the others modes because of the presence of the pad that has two roles in the coupling mechanism:

- it is considered as a lumped stiffness in the out-of -plane direction (z): the value of this stiffness is k_n;
- it is a single degree of freedom in the in-plane direction (x), that is coupled with the out-of-plane vibrations of the disc and the beams through the friction force.

The out-of-plane dynamics of the laboratory brake is described by the system stiffness matrix $\mathbf{K}_0$ and the system mass matrix $\mathbf{M}_0$.

[1] A modal analysis software developed at the Imperial College.

[2] Generally the two matrices related to the double modes of the disc do not have the same dimensions: first, because the $(n,0)$ modes are not double modes; second, because, due to the non-symmetric disc constraints, some of the disc modes can split in uncoupled conditions. The matrices, denoted with the subscript $d1$, contain the modes which are not repeated and one set of the repeated mode. The matrices with the subscript $d2$ contain the second set of repeated modes.

Eq. (1) shows the uncoupled system matrices $\mathbf{M}_0$ and $\mathbf{K}_0$, that describes the system when there is no contact between disc and pad.

These matrices are obtained by expanding the stiffness matrices $\mathbf{\Lambda}_{d1}$ and $\mathbf{\Lambda}_{d2}$ of the disc and $\mathbf{\Lambda}_b$ of the beam; the beam stiffness matrix ($\mathbf{\Lambda}_b$) is repeated twice because there are two beams, one on each side of the disc. The first N_d rows are related to the degrees of freedom of the disc, the rows between $N_{d1}+1$ and $N_{d1}+N_{d2}$ to the double modes of the disc, the next N_b to the first beam, the following N_b to the second beam. The dimension of the system matrix is therefore $N_s = N_{d1} + N_{d2} + 2N_b$.

$$\mathbf{K}_0 = \begin{bmatrix} \begin{bmatrix} \ddots & & \\ & \mathbf{\Lambda}_{d1} & \\ & & \ddots \end{bmatrix} & 0 & 0 & 0 \\ 0 & \begin{bmatrix} \ddots & & \\ & \mathbf{\Lambda}_{d2} & \\ & & \ddots \end{bmatrix} & 0 & 0 \\ 0 & 0 & \begin{bmatrix} \ddots & & \\ & \mathbf{\Lambda}_b & \\ & & \ddots \end{bmatrix} & 0 \\ 0 & 0 & 0 & \begin{bmatrix} \ddots & & \\ & \mathbf{\Lambda}_b & \\ & & \ddots \end{bmatrix} \end{bmatrix}, \quad \mathbf{M}_0 = \begin{bmatrix} \begin{bmatrix} \ddots & & \\ & \mathbf{I} & \\ & & \ddots \end{bmatrix} & 0 & 0 & 0 \\ 0 & \begin{bmatrix} \ddots & & \\ & \mathbf{I} & \\ & & \ddots \end{bmatrix} & 0 & 0 \\ 0 & 0 & \begin{bmatrix} \ddots & & \\ & \mathbf{I} & \\ & & \ddots \end{bmatrix} & 0 \\ 0 & 0 & 0 & \begin{bmatrix} \ddots & & \\ & \mathbf{I} & \\ & & \ddots \end{bmatrix} \end{bmatrix} \tag{1}$$

The modes of the disc and the beams are coupled together through the out-of-plane stiffness k_n of the pad.

The elastic force acting on the disc, due to relative displacement between disc and beam, can be written as:

$$F_e = k_n(z_d - z_b)\delta(x - x_0)\delta(y - y_0) \tag{2}$$

and the modal force F_i^m acting on the i^{th} mode of the disc is:

$$F_i^m = \iint_d \Phi_i F_e \,\mathrm{d}x\,\mathrm{d}y = \iint_d \Phi_i k_n(z_d - z_b)\delta(x - x_0)\delta(y - y_0)\,\mathrm{d}x\,\mathrm{d}y = \Phi_i^P k_n(z_d - z_b), \tag{3}$$

where Φ_i is the i^{th} mode of the uncoupled disc; z_d and z_b are the out-of-plane physical displacements of the disc and beam, respectively, and δ the Dirac function. Φ_i^p is the mode evaluated at the contact point $P(x_0,y_0)$.

The displacements of the disc and the beams can be expressed as a linear combination of the modal displacements so that:

$$F_i^m = \Phi_i^P k_n \left(\sum_{i=1}^{N_b} \Psi_i^P p_i - \sum_{i=1}^{N_{d1}} \Phi_i^P q_i \right), \tag{4}$$

where Ψ_i^p is the ith mode of the beam, p_i and q_i are the modal displacements of the disc and the beam, respectively, and N_d and N_b are the number of modes of the disc and the beam, included in the model. These elements are not diagonal anymore and form the coupling system stiffness matrix $\mathbf{K}$:

$$\begin{aligned} K_{i,j} &= \Phi_i^P k_n \Phi_j^P \quad \forall 1 < i < N_d, \quad 1 < j < N_d, \\ K_{i,j+N_{d1}+N_{d2}} &= -\Phi_i^P k_n \Psi_j^P \quad \forall 1 < i < N_d, \quad 1 < j < N_b. \end{aligned} \tag{5}$$

The experimental results show a strong sensitivity to the misalignment angle between the disc and the beam. To take into account such angle α, as shown in Fig. 2(a), the coupling elements in the system stiffness matrix become:

$$\begin{aligned} K_{i,j} &= \Phi_i^P k_n \Phi_j^P \quad \forall 1 < i < N_d, \quad 1 < j < N_d, \\ K_{i,j+N_{d1}+N_{d2}} &= -\Phi_i^P k_n \Psi_j^P \cos(\alpha) \quad \forall 1 < i < N_d, \quad 1 < j < N_b. \end{aligned} \tag{6}$$

The other coupling terms are added in the same way.

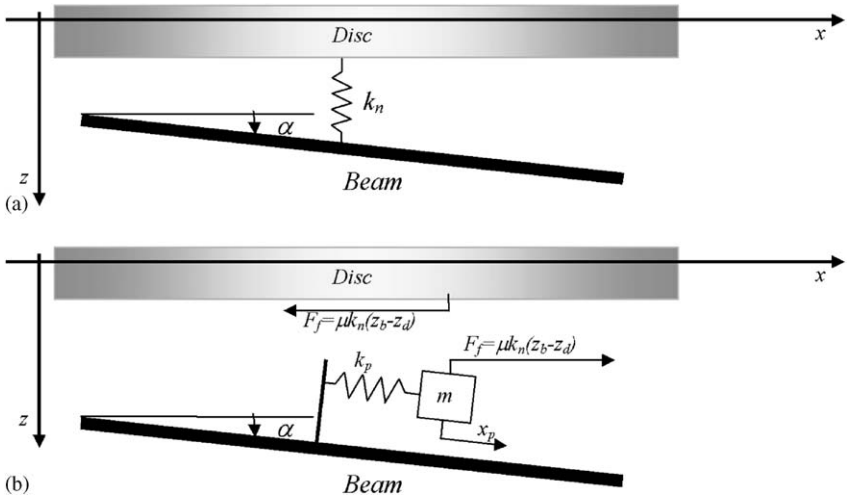

Fig. 2. Out-of-plane model of the pad (a), in-plane model of the pad (b).

The coupled system is described by a new matrix **K***, i.e.:

$$\mathbf{K}^* = \mathbf{K}_0 + \mathbf{K}. \tag{7}$$

The model is now able to describe the out-of-plane dynamics of the set-up; this model is valid until the deformed shape of the coupled system can be described as a linear combination of the modes of the disc and the beams in uncoupled conditions, i.e. when the coupling conditions are not too strong.

To model the friction interaction a further expansion of the model is necessary.

In the in-plane direction the pad is modeled as a one degree of freedom system, as shown in Fig. 2(b). The direction of the degree of freedom x_p is parallel to the beam axis.

For each of the two pads the following equation can be written:

$$m\ddot{x}_p + k_p x = F, \tag{8}$$

where m is the mass of the pad and k_p its tangential stiffness.

By adding two extra degrees of freedom, one for each pad, the system matrices **K** and **M** are expanded into the matrices **K**′ and **M**′.

$$\mathbf{K}' = \begin{bmatrix} \begin{bmatrix} & \mathbf{K}^* & \end{bmatrix} & 0 \\ 0 & \begin{bmatrix} k_p & 0 \\ 0 & k_p \end{bmatrix} \end{bmatrix}, \quad \mathbf{M}' = \begin{bmatrix} \begin{bmatrix} & \mathbf{M} & \end{bmatrix} & 0 \\ 0 & \begin{bmatrix} m & 0 \\ 0 & m \end{bmatrix} \end{bmatrix}. \tag{9}$$

The vibrations of the pad are coupled with the transverse vibrations of the disc and the beams, primarily by the friction force. The friction force is modeled by the Coulomb law and μ is assumed to be constant; it is also assumed, based on the experimental results presented in Ref. [19], that the sliding velocity between disc and pads is always higher than the maximum velocity of vibration of the pad, implying that there is no stick-slip motion arising. These considerations lead to a linear model of the friction interaction between disc and pad. The normal force is the elastic force, i.e. proportional to the relative displacement between disc and beam. The friction force F_f is:

$$F_f = \mu F_N = \mu k_n (z_d - z_b \cos(\alpha)) \cos(\alpha), \tag{10}$$

where z_d and z_b are the out-of-plane displacements of the disc and the beam at the contact point, respectively, and can be expressed as a linear combination of the disc and beam modes:

$$F_f = \mu k_n \left(\sum_{i=1}^{N_{d1}} \Phi_i^P q_i - \sum_{i=1}^{N_b} \Psi_i^P p_i \cos(\alpha) \right) \cos(\alpha). \tag{11}$$

These terms, coming from the friction interaction between disc and pad, are non-symmetric.

Other coupling terms derive from the misalignment force F_m, due to the angle α:

$$F_m = k_n \left(\sum_{i=1}^{N_{d1}} \Phi_i^P q_i - \sum_{i=1}^{N_b} \Psi_i^P p_i \cos(\alpha) \right) \sin(\alpha). \tag{12}$$

These terms are symmetric and, if the angle α is small, they are considered negligible with respect to those due to the friction force.

The coupling terms for the first pad in the expanded system matrix $\mathbf{K}'$ are:

$$\begin{aligned} K'_{i,j} &= -k_n \Phi_j^P (\mu \cos(\alpha) + \sin(\alpha)) \quad \forall i = N_s + 1, \quad 1 < j < N_d, \\ K'_{i,j+N_{d1}+N_{d2}} &= k_n \Psi_j^P (\mu \cos(\alpha) + \sin(\alpha)) \cos(\alpha) \quad \forall i = N_s + 1, \quad 1 < j < N_b, \end{aligned} \tag{13}$$

where N_s is the dimension of the system matrix $\mathbf{K}$.

The terms due to the misalignment angle are symmetric, and represent the terms that couple back the vibration of the pads with the out-of-plane vibrations of the disc and the beams:

$$\begin{aligned} K_{i,j} &= -k_n \Phi_i^P \sin(\alpha) \quad \forall 1 < i < N_d, \quad j = N_s + 1, \\ K'_{i+N_{d1}+N_{d2},j} &= k_n \Psi_i^P \sin(\alpha) \cos(\alpha) \quad \forall 1 < i < N_b, \quad j = N_s + 1. \end{aligned} \tag{14}$$

In the same way the terms related to the second pad are coupled with the vibration of the disc and the beams.

Both the normal stiffness k_n and the in-plane stiffness k_p are complex to model the hysteretic damping of the friction material (i.e. $k_p = k_p^*(1+j\eta)$ and $k_n = k_n^*(1+j\eta)$).

2.1. Discussion of the model

The proposed model accounts for the out-of-plane dynamics of the laboratory brake through the uncoupled bending modes of the disc and the beams that can be accurately measured. Since these measurements are performed in uncoupled condition, i.e. when disc and beams are not in contact, the modes are not affected by any uncertainty or nonlinearity related to the pad. The in-plane dynamics of the disc is not included in the model because it was verified that the first rotational mode of the disc is around 800 Hz and falls below the frequency range of interest, while the other rotational modes are above 10 kHz. Also, during the experiments, squeal occurred only at frequencies corresponding to bending modes of the disc or the beams. At these frequencies the in-plane vibrations of the disc are negligible with respect to the out-of-plane ones.

The small brake pad is modeled in the out-of-plane direction by a stiffness connection between the disc and the beams; such simplification is acceptable because the wavelengths related to the squealing bending modes are much larger than the length of the pad.

The dynamic characteristics of the pad in the model are its mass m, the out-of-plane stiffness k_n, and its in-plane eigenfrequency. Appendix A provides insight on the evaluation of these parameters. However, it is important to notice that the value of k_n is primarily affected by the chosen angle of attack, the geometry of contact area, the thickness of the pad; also temperature and wear may affect its value. Therefore the authors decided, instead of accounting for all these effects, to perform a measurement to estimate the order of magnitude of k_n. The used procedure provides a value for this stiffness within an error of 50%. Although the

error is significant, it is accepted because it bounds the error between the experimental natural frequencies and the eigenvalues of the model within 5%.

The measurements reported in Ref. [19] show that the in-plane dynamics of the pad plays a key role in the selection mechanism of the squealing mode. In fact, any squealing mode falls close to a natural frequency of the pad. The experimental analysis shows also that the in-plane natural frequencies of the pad are significantly affected by:

- the normal load, that causes a variation of the eigenfrequencies of the pad up to 25%;
- the wear of the pad: brand new pads present usually several eigenfrequencies, while used pads have only one major peak in the frequency response. This peak shifts toward higher frequencies when the wear increases;
- the angle of attack, that causes a variation of the eigenfrequencies of the pad up to 15%;
- the dimension of the pad.

To resume, the experiments on the laboratory brake show that, if a mode is squealing, there is always an in-plane mode of the pad close to the squealing mode. Changing the operational parameters, it is possible to move an in-plane mode of the pad to any frequency between 800 Hz and 12 kHz. Therefore, it is convenient to perform the complex eigenvalue analysis in function of the in-plane eigenfrequency of the pad.

A last consideration concerns the contact law: in the literature many authors use a constant friction coefficient and the assumption of no stick-slip behavior [8,9,13,15,21,23]. The authors performed appropriate measurements to verify if this hypothesis can be applied to the laboratory brake model. The experimental results in Ref. [19] show that, during the squeal limit cycle, the maximum in-plane velocity is between 30% and 50% of the average rotational velocity of the disc. This difference assures that measurement errors or variation in the rotational velocity would not cause any change in the direction of the relative velocity. Moreover, the onset of instability occurs when the in-plane vibration of the pad is two orders of magnitude lower than the amplitude of the squeal limit cycle, implying that the onset of instability can develop in non-stick-slip conditions.

On the contrary, for low rotational velocities, a stick-slip limit cycle can occur but the frequency of this cycle is hundred times slower than the squeal limit cycle[3].

2.2. Results from the reduced order model

The stability of the model is derived by a complex eigenvalue analysis. Multiple extraction of the eigenvalues are performed for different values of the in-plane eigenfrequencies of the pad that ranges between 2 and 10 kHz.

Fig. 3 shows the result of the analysis for an angle of attack $\alpha = -1^{\circ}$; the horizontal lines are the modes of the disc and the beams[4]. the disc and/or beam modes are affected by the variation of the natural frequency of the pad only if they are close to the mode of the pad. When the eigenfrequency of the pad (the diagonal line) crosses some of the disc or beam eigenfrequencies, the real part of the eigenvalue becomes positive. A negative damping is assumed as the onset of squeal occurrence and the unstable points are marked as black lines in the graph.

Table 1 lists the experimental results indicating which modes of the laboratory brake may squeal and the corresponding results from the complex eigenvalue analysis performed with the model.

The simulation shows a good agreement with the experimental results in the frequency range where the model is applicable. The last two squealing modes are not included in the model because of the limited bandwidth of the exciting hammer during modal tests.

[3]The stick slip can cause low frequency brake noises like creep, groan, and moan, that are not the aim of the present work.

[4]The eigenvalues of the model represent the modes of the coupled system. However, since the coupling between disc and beams is not strong, it is possible to recognize the deformed shape of the original uncoupled modes. In the following, when referring to the modes of the disc, a mode of the coupled system, characterized by large vibrations of the disc and negligible vibrations of the rest of the system (the beams and the pads), is considered. Similarly, the same meaning holds for the beam and pad modes. When in coupled conditions, the double modes of the disc are split: the label $(n,m-)$ refers to the mode having an antinode in the contact position, while the label $(n,m+)$ refers to the mode with an antinode.

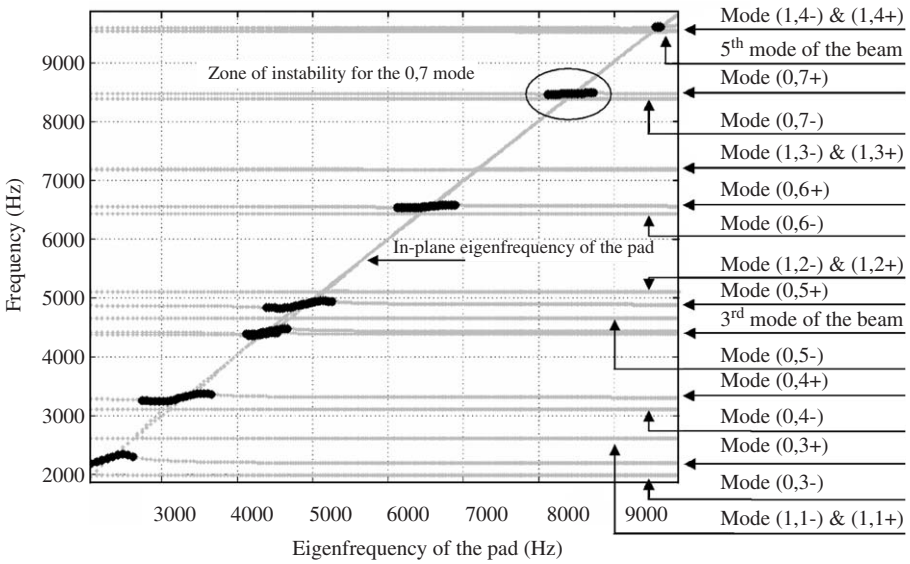

Fig. 3. Complex eigenvalues analysis for $\alpha = -1^{\circ}$.

Table 1
Comparison between experimental and simulated results

Squealing mode	Squeal frequency (experimental) (Hz)	Squeal frequency (reduced model) (Hz)
(0,3+) Disc	2005	2100
(0,4+) Disc	3100	3150
3rd Beam	4300	4400
(0,5+) Disc	4700	4900
(0,6+) Disc	6400	6550
(0,7+) Disc	8400	8450
5th Beam	9489	9600
(0,8+) Disc	10 400	NA
(0,9+) Disc	12 400	NA

Fig. 4 shows the detail of the unstable zone related to the mode (0,6+) on the complex plane. (The real part is scaled to represent the percentage damping and the imaginary part to represent the frequency.) Four coupled system modes fall in this frequency range:

- the (0,6−) mode of the disc that is not affected by the dynamics of the pad because its amplitude at the contact point is zero;
- the (0,6+) mode, the unstable mode, that involves mainly the vibration of the (0,6+) disc mode and the two degrees of freedom of the pads;
- the two modes of the pads: these two modes couple the vibration of the two in-plane degrees of freedom of the pads. The first one is characterized by the two pads moving in phase, while the second one has the two pads vibrating in phase opposition.

By an analysis of the eigenvectors of the squealing mode it is possible to see that the squealing mode is characterized by:

- the two pads moving in phase opposition;
- a 90° phase between the disc mode and the pads vibration.

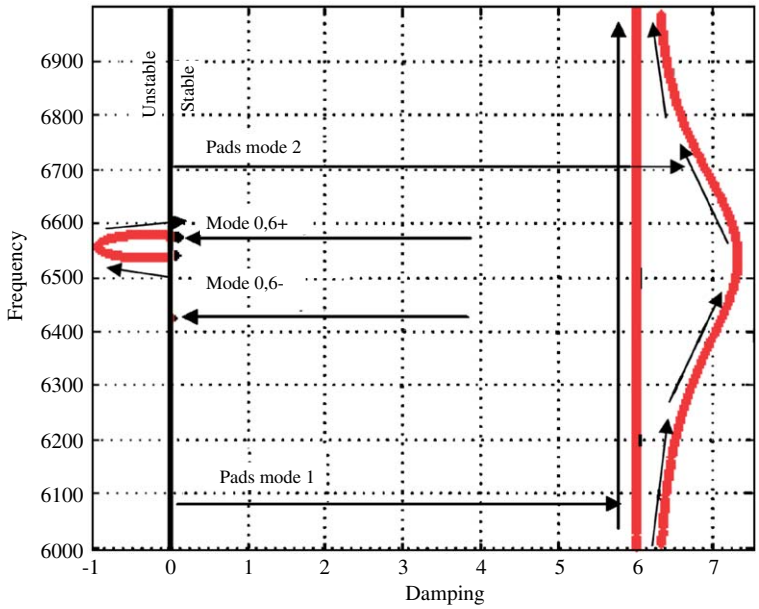

Fig. 4. Locus plot related to the (0,6+) mode instability.

This result is in agreement with the experiments [19] that show that the phase shift between the bending modes of either the disc or the beams and the in-plane mode of the pad is an emerging characteristic of the squeal behavior of the laboratory brake.

The locus plot in Fig. 4 highlights an instability mechanism arising in the laboratory brake, described by the suggested model, that is consistently different from the standard mode-lock-in characteristics presented in the literature [15,20–22]. The eigenvalues of the system do not coalesce in the complex eigenvalue analysis because of the large difference between the real parts of the eigenvalues of the disc and the beams with respect to the real part of the in-plane eigenfrequency of the pads. Nevertheless, the mode (0,6+) and the pad mode-2 influence each other: when the latter moves toward higher damping values, it destabilizes the first one, pushing it into the unstable zone. Because of the distance between the eigenvalues, the frequency of the unstable eigenvalue does not change too much.

To study the influence of the in-plane damping on the interaction between pad and system modes, a model with a lower damping is considered.

Fig. 5 shows how, changing the 6% damping of the model (Fig. 4), that is experimentally evaluated, down to 0.1%, the interaction between the eigenvalues presents the mode lock-in and lock-out characteristic [15,20–22], even if the presence of the structural damping in the disc and beam modes does not permit the eigenvalues to coalesce completely. In this case the lock-in and lock-out points become an area where the imaginary parts of the eigenvalues become close, while the real parts split: the mode of the pad moves toward the positive half plane, while the mode (0,6+) becomes unstable.

Basically, the lock-in characteristics presented in the beam-on-disc models [20–22] reflect an interaction between structures that are lightly damped or undamped; lock-in occurs differently in damped structures. The most relevant difference is that there is no need of exact coincidence between the in-plane eigenfrequency of the pad and a bending mode of the disc to have an unstable behavior. On the contrary, there is a frequency range around the in-plane eigenfrequency of the pad where instability of other modes may occur, and this zone become wider as the in-plane damping increases. (This consideration leads to the necessity of introducing the squeal index B, that is defined in the last part of the paper.)

Running the complex eigenvalue analysis for many values of the angle of attack, it is possible to describe the zone of instability on an angle–frequency graph. Fig. 6 shows the comparison between the zones of instability found by the reduced order model and the squeal points found during the experiments.

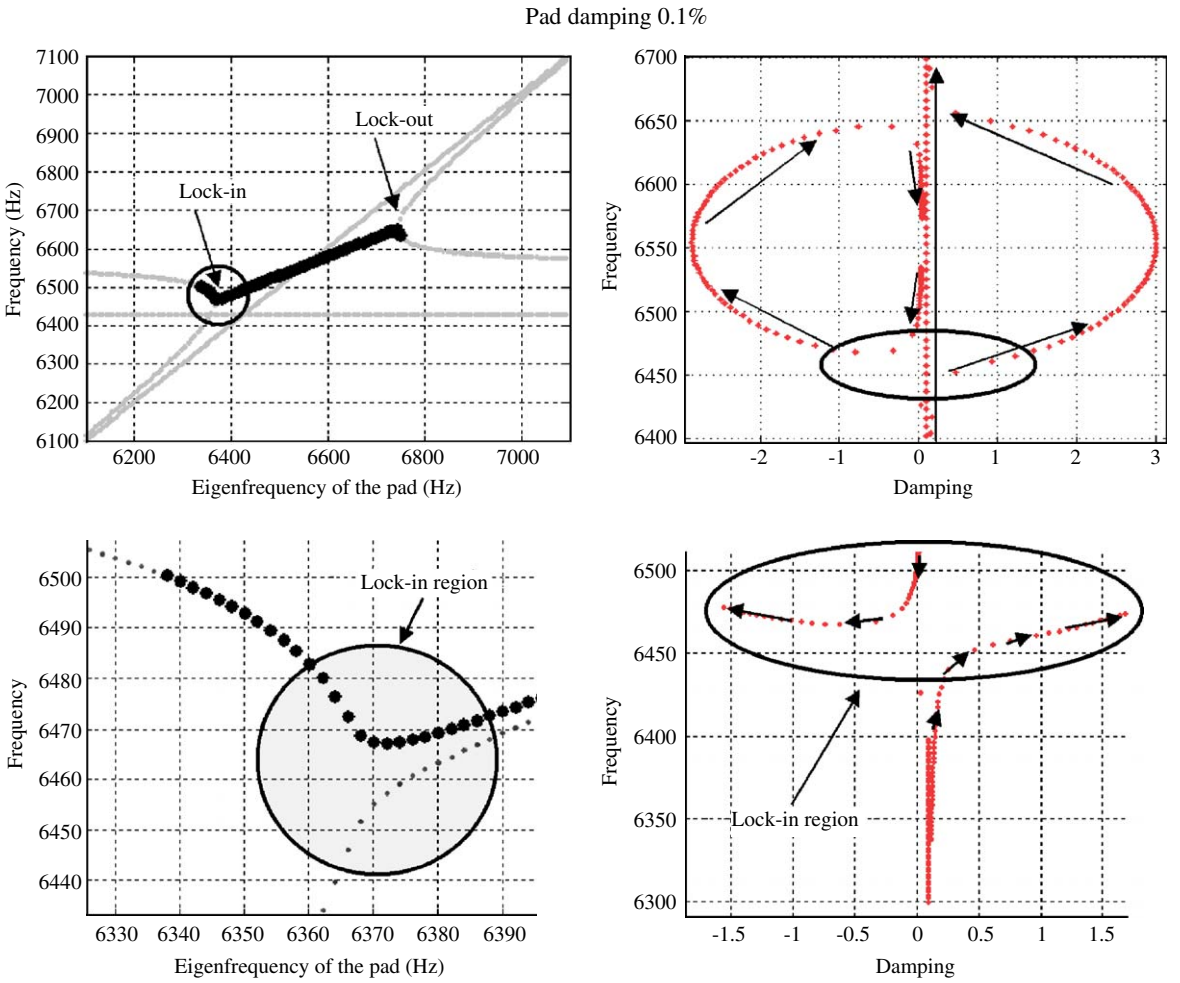

Fig. 5. Influence of damping in the eigenvalues interaction.

The model shows a good agreement with the experimental data for negative values of the angle of attack, but does not show any instability when such angle is close to zero or when it is positive.

2.3. *Modeling the brake pad by a 1-degree of freedom rotational system*

The comparison between the results from the model and the experimental results highlights the need for an improvement of the model of the pad. If the angle of attack is positive another squeal mechanism can occur involving the coupling of a rotational mode of the pad with the bending modes of the disc or the beams. Therefore a rotational degree of freedom of the pad must be added to the model. The parameters characterizing the new model are (Fig. 7):

– the moment of inertial J of the pad with respect to its center of mass;
– the geometrical characteristics of the pad: length l and height h;
– the characteristic stiffness of the pad, represented by a rotational stiffness k_p;
– the rotational degree of freedom θ;
– the center of normal interaction between disc and pad, that is at a distance l_c from the center of the pad.

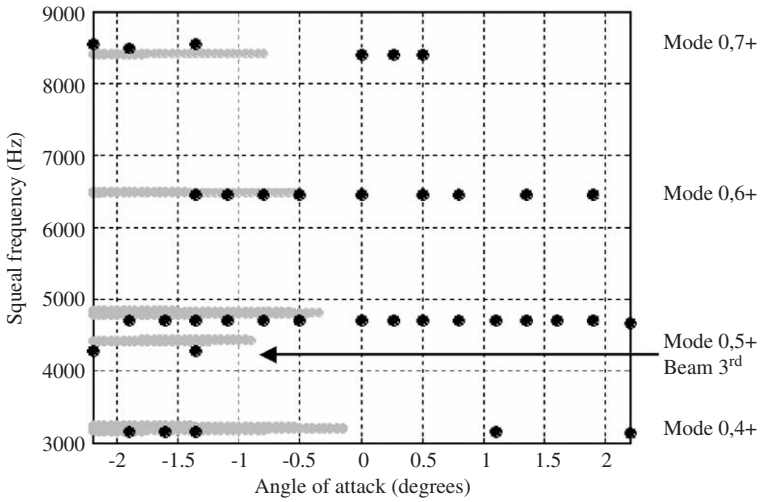

Fig. 6. Instability map: comparison between experimental (black dots) and numerical results (grey area).

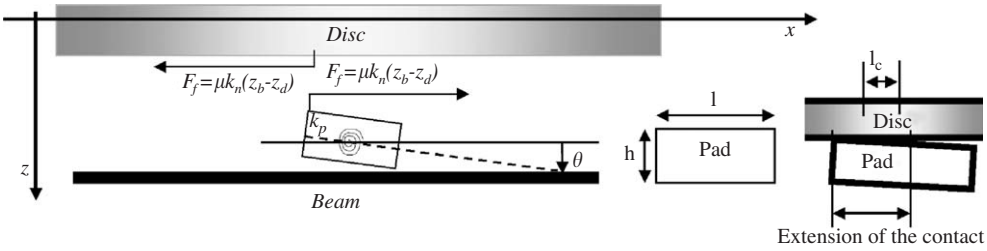

Fig. 7. Rotational model of the pad.

The pads are assumed to rotate initially because of the angle of attack (positive) or because of the effect of the friction force (if the angle is zero). Therefore the contact area between the disc and the pad becomes smaller and non-symmetric with respect to the center of the pad. The normal force between disc and pad is applied in the center of the contact area, which is at a distance l_c from the center of the pad.

Since the rotational and the translational modes of the pad do not interact, it is possible, for a sake of simplicity, to consider the two models separately: using the rotational degree of freedom for positive angles of attack and the translational degree of freedom only for negative angles.

Therefore Eq. (9) can be rewritten as follows:

$$\mathbf{K}' = \begin{bmatrix} \begin{bmatrix} & \mathbf{K}^* & \\ & & \end{bmatrix} & 0 \\ 0 & \begin{bmatrix} k_r & 0 \\ 0 & k_r \end{bmatrix} \end{bmatrix}, \quad \mathbf{M}' = \begin{bmatrix} \begin{bmatrix} & \mathbf{M} & \\ & & \end{bmatrix} & 0 \\ 0 & \begin{bmatrix} J & 0 \\ 0 & J \end{bmatrix} \end{bmatrix}, \tag{15}$$

where k_r is the rotational stiffness, and J the moment of inertia of the pad. The friction force produces a torque M_f on the pad that is:

$$M_f = F_f h/2 = \mu F_N h/2 = \mu k_n (z_d - z_b \cos(\alpha)) h/2. \tag{16}$$

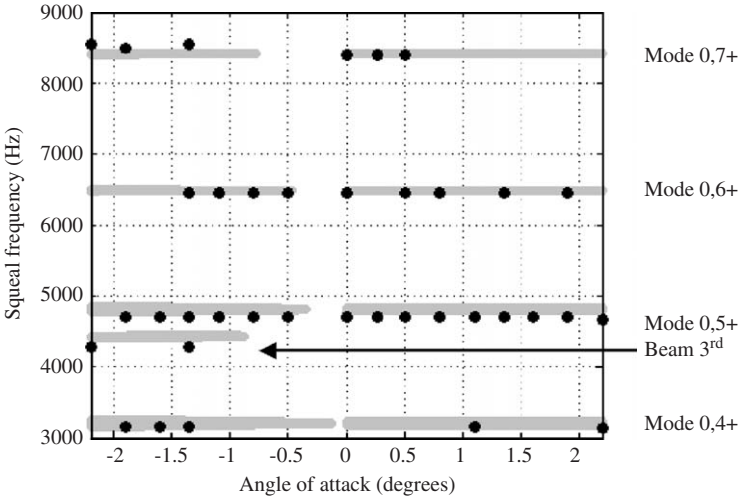

Fig. 8. Instability map: comparison between experimental (black dots) and numerical (grey) results.

It can be also expressed in terms of the modal coordinates as follows:

$$M_f = \mu k_n \left(\sum_{i=1}^{N_{d1}} \Phi_i^P q_i - \sum_{i=1}^{N_b} \Psi_i^P \cos(\alpha) p_i \right) h/2. \tag{17}$$

The terms in the system stiffness matrix are:

$$\begin{aligned} K'_{i,j} &= -\mu k_n \Phi_j^P h/2 \quad \forall i = N_s + 1, \quad 1 < j < N_d, \\ K'_{i,j+N_{d1}+N_{d2}} &= \mu k_n \Psi_j^P h \cos(\alpha)/2 \quad \forall i = N_s + 1, \quad 1 < j < N_b, \end{aligned} \tag{18}$$

when assuming the normal stiffness lumped in the center of the normal reaction between disc and pad. The feedback force, i.e. the force that the rotation of the pad applies to the disc and the beam, can be expressed as:

$$\begin{aligned} K'_{i,j} &= k_n \Phi_i^P l_c \quad \forall 1 < i < N_d, \quad j = N_s + 1, \\ K'_{i+N_{d1}+N_{d2},j} &= -k_n \Psi_i^P \cos(\alpha) l_c \quad \forall 1 < i < N_b, \quad j = N_s + 1. \end{aligned} \tag{19}$$

The terms in Eq. (19) are symmetric. When the disc is deformed, the stiffness k_n causes a torque on the pad:

$$\begin{aligned} K_{i,j} &= k_n \Phi_i^P l_c \quad \forall i = N_s + 1, \quad 1 < j < N_d, \\ K'_{i,j+N_{d1}+N_{d2}} &= -k_n \Psi_i^P \cos(\alpha) l_c \quad \forall i = N_s + 1, \quad 1 < j < N_b. \end{aligned} \tag{20}$$

By comparing Eq. (19) with Eq (14), that express the feedback terms for the two models, it is possible to notice that the terms in Eq. (20) are not zero if $\alpha = 0$, Therefore the rotational model can produce instability even if the angle of attack is zero.

Using the two proposed models together it is possible to obtain the stability map in Fig. 8, where the experimental results and the simulated ones are in agreement for all the angles of attack.

This new rotational model confirms the original idea and the established aim of this study: a correct model of the squeal instability in a real brake can be achieved through subsequent modifications and improvements of the laboratory set-ups. The modeling of such set-ups should establish which part of previous models can be maintained and what must be improved or corrected.

3. The squeal indexes

Since the reduced order model is able to predict the squeal behavior of the laboratory brake, it is possible to use the model to estimate also the sensitivity of squeal to parameters variations in the model. To explore the sensitivity of the squeal a measure of the instability level is needed. Thus, two different squeal indexes are proposed for this purpose.

The results from the model show that, when the eigenfrequency of the pad approaches some of the eigenfrequencies of the system, the corresponding mode may become unstable because the real part of the eigenvalue moves from the negative to the positive region of the complex plane.

For the following consideration, a single mode of the system, e.g. the (0,6+) mode of the disc at 6485 Hz, is considered and a complex eigenvalue analysis as a function of the eigenfrequency of the pad is performed.

When the eigenfrequency of the pad approaches the disc natural frequency, the effective damping drops, from 0.02%, the modal damping of the (0,6+) mode, down to zero and becomes negative. Fig. 9 shows the effective damping of the eigenvalue as a function of the in-plane eigenfrequency of the pad. To describe the stability region of this mode, two distinct indexes can be suitably defined.

The first one, named Squeal Index A (SI_A), is proportional to the maximum negative amplitude of the damping. This index is the effective percentage damping defined as:

$$SI_A = \left|\mathrm{Re}(\lambda)/\mathrm{Im}(\lambda)\right| 100, \tag{21}$$

where λ is the complex eigenvalue of the selected mode of the model.

The squeal index A gives information on the robustness of the squeal to damping variations.

Because there is a range of values for the eigenfrequency of the pad that leads to instability, the second index, named squeal index B (SI_B), is proportional to the range of frequency Δf where instability occurs and is defined as:

$$SI_B = \Delta f / f_c 100, \tag{22}$$

where f_c is the central frequency of the band Δf.

This index provides an estimation of the robustness of the squeal to variations of the modal parameters of both disc and pad.

For a squeal event to occur it is necessary that both the indexes be positive; moreover a mode with larger values of the indexes is more likely to squeal.

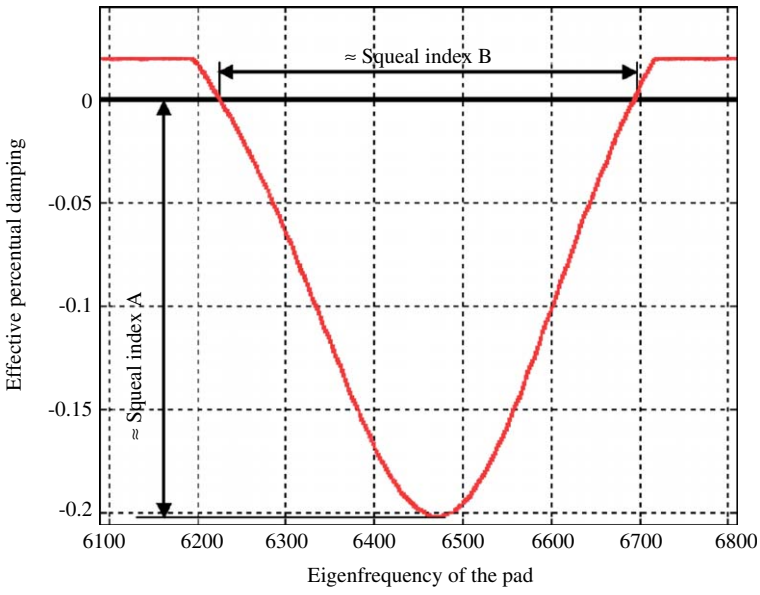

Fig. 9. Effective damping of the eigensolution.

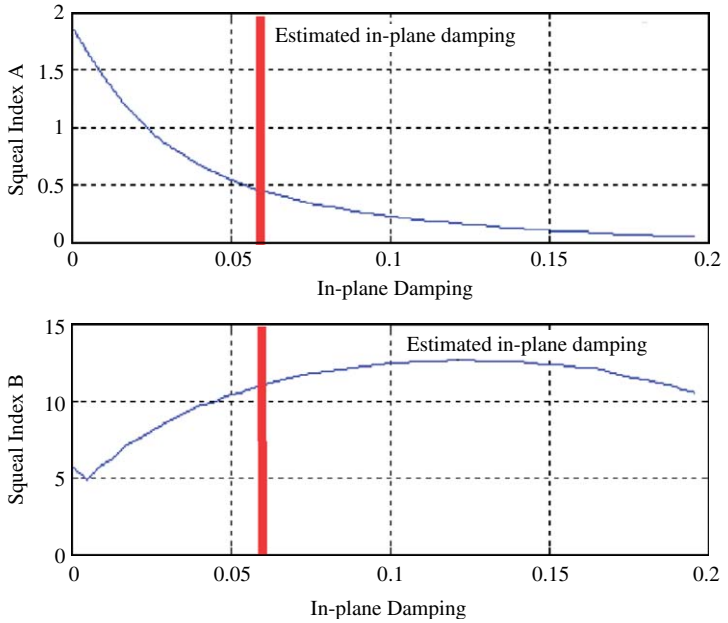

Fig. 10. Squeal indexes as a function of the in-plane damping.

It is possible to perform several complex eigenvalue analyses, changing each time one of the parameters of the model and, for each test, to extract the trend of these two indexes.

Starting from the nominal values of the parameters of the model the squeal indexes increase if either the normal stiffness or the friction coefficient μ increase; vice-versa, as expected, the out-of-plane damping of the pad is a squeal inhibitor and the squeal indexes decrease when it increases.

It is important to notice that the effective negative damping is −4.8% for the nominal values. This value is much higher than the structural damping of the beam and the disc that, depending on the mode, is around 0.5%. Therefore, to suppress the squeal by adding passive damping, it is necessary to reach, for each of the squealing modes, a 5% modal damping. The squeal index B is, for the nominal value, around 11%, implying that the squeal can still occur even if either the mode (0,6) or the in-plane eigenfrequency of the pad has a 10% variation in frequency.

Fig. 10 shows the behavior of the indexes for a variation of the in-plane damping: as expected, the index A decreases when the damping increases but the index B shows a zone of increasing tendency to squeal when the damping increases.

This unexpected result provides a key information on the squeal behavior. The in-plane damping, while reduces the robustness of the squeal with respect to damping variations, increases the range of frequencies of the pad that can lead to squealing behavior. This double role of the damping should be kept in mind during the design process of the brake and the damping should be added, if possible, only in the out-of-plane direction.

Finally, one should be aware that the brake production and assembly process causes a wide variation of all the parameters of the brake apparatus, so that the boundary of the stability region is not properly a line but rather a sub-region where the squeal, under certain circumstances and for certain realizations, can occur. For this reason the squeal index B is the most relevant parameter because it provides a measure of the robustness of the brake apparatus to variations of the dynamic properties.

4. Conclusions

This paper presents a possible approach to the comprehension and solution of the brake squeal problem based on a series of steps of experimentation and modeling. At each step, a more complex ''brake like'' set-up is analyzed experimentally, and a predictive model is built.

This work represents a successful first step: in fact, the reduced model proposed in this paper is able to predict all, and only, the squeal frequencies that occur during the experiments performed on the laboratory brake set-up. Moreover, in agreement with the experimental results, the model predicts squeal occurring at the natural frequencies of the disc or the beam only if the in-plane eigenfrequency of the pad falls close to it. The unstable eigenvector, as well as the experimental squealing modes, are complex, and the in-plane vibrations of the pad have a 90° phase shift with respect to the out-of-plane vibration of the disc and the beam. Finally, the results from the model are able to capture the dependency between squeal frequency and angle of attack of the beams.

As a result, the onset of the instability and several other aspects of the squeal vibrations can be obtained from a linear model of the brake. Therefore, it is possible to state that the nonlinear aspects related to the contact between disc and pad, e.g. non constant friction coefficient, stick-slip or detachments, material nonlinearities, etc., do not cause squeal occurrence while, on the contrary, they are the mechanisms that can stabilize the squeal vibrations on a limit cycle.

The linear model can also provide indexes of the squeal tendency of the set-up. To this purpose two different indexes are proposed, the SI_A, estimating the robustness of the squeal to structural damping variations, and the SI_B that provides a measure of the range of destabilized frequencies. The analysis of the dependence of the squeal indexes shows that, as expected, the squeal tendency increases by increasing either the friction coefficient or stiffness of the pad, while it decreases by increasing the out-of-plane damping. This analysis shows also that the in-plane damping on the pad, while it reduces the severity of the squeal, increases the parameter range for which instability may occur.

To conclude, the model highlights that the squeal mechanism is driven mainly by three factors:

1. the friction force that induces asymmetry in the stiffness matrix. This is a characteristic exhibited by every friction law because the friction couples together normal and tangential forces;
2. the resonance of the pad, that induces a 90° phase shift between the friction force and the displacement of the pad, when the natural frequency of the pad falls close to a natural frequency of the system (disc or beams);
3. the feedback force that couples the in-plane vibration of the pad with the bending modes of the disc and the beams. This force is in phase with the displacement of the pad; thus, it has 90° phase difference with respect to the out-of-plane displacement of the disc or the beams. The feedback force can be caused by the misalignment angle as well as by rotational modes of the pad.

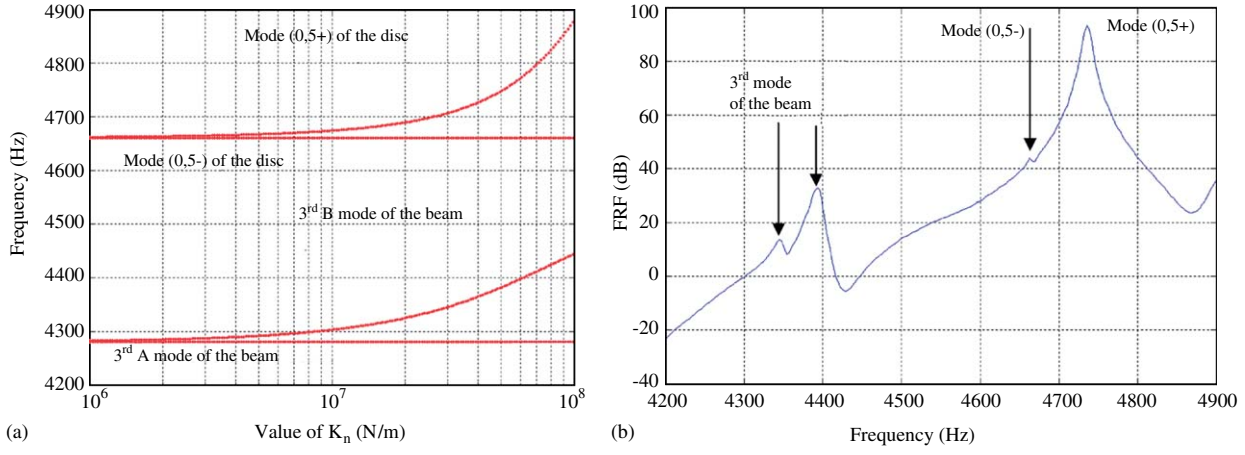

Fig. 11. Split of the eigenvalues of the model (a), experimental FRF of the laboratory brake (b).

Appendix A. Experimental evaluation of the parameters of the pad

The model of the pad needs the evaluation of few parameters that are the normal stiffness k_n, the mass m, and the damping loss factor η. Appropriate experimental procedure are here presented.

The pads used in the laboratory brake have a contact area equal to $1\,cm^2$ and is made with brake friction material; the height of the pad is 0.5 cm. An experimental estimation of the normal stiffness of the pad is necessary because the results of the model are sensitive to this parameter. Also, the material properties of the brake pad are generally unknown and, because of the contact stiffness, the effective stiffness of the pad is generally one order of magnitude lower than the calculated one.

The contact between disc and beam through the pad causes the disc to lose its symmetry so that the double modes of the disc split. The split between them depends on the normal stiffness of the pad; therefore it is possible to estimate k_n from a measure of the mode split.

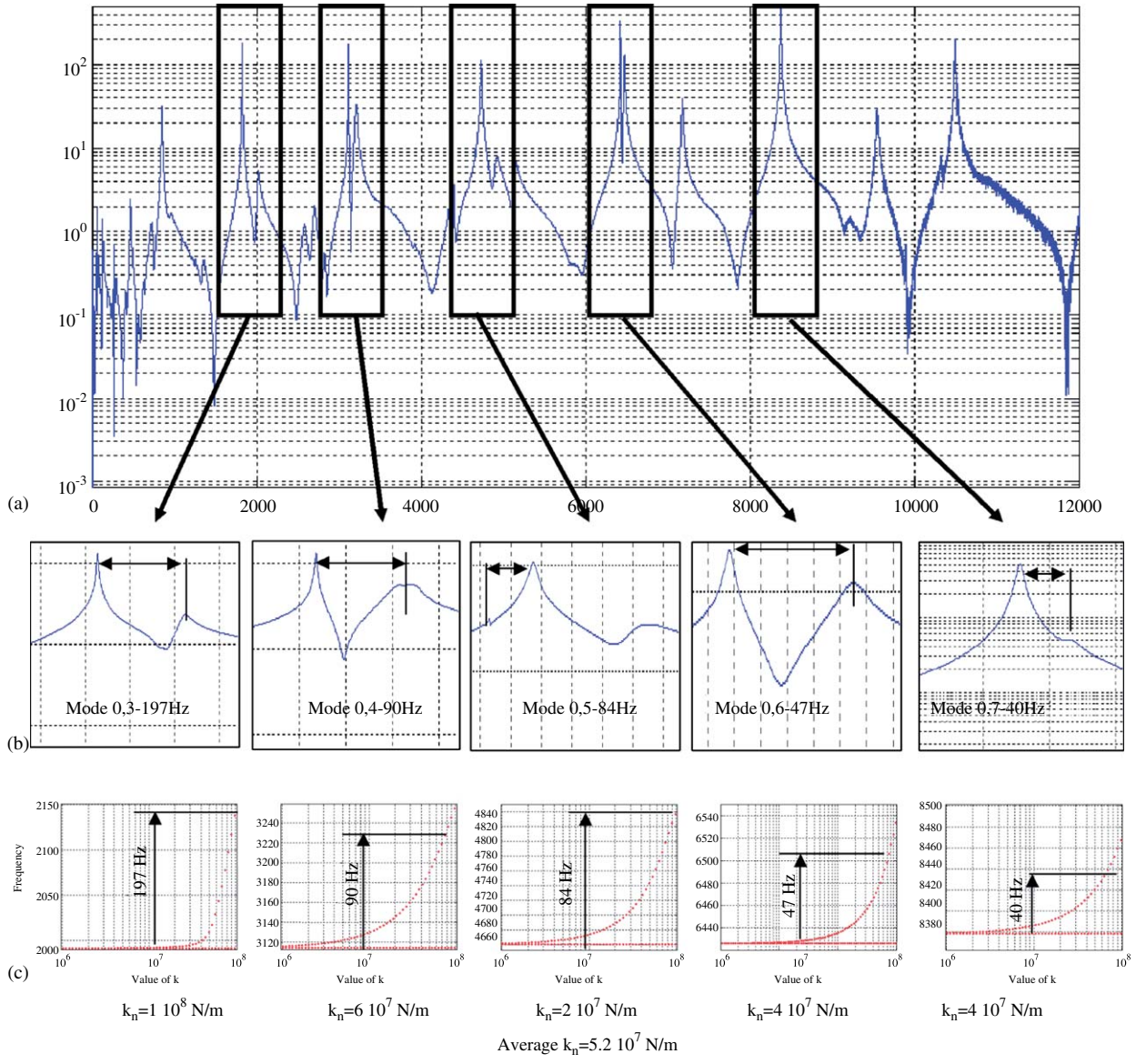

Fig. 12. Evaluation of k_n: FrF of the coupled system (a), split between double modes of the disc (b), split between eigenvalues of the model (c).

Fig. 11 (a) shows the eigenvalues of the model in the frequency range between 4000 Hz and 5200 Hz.The eigenvalues of the system are plotted as a function of the normal stiffness k_n. Fig. 11(b) shows the frequency response function of the laboratory brake in the considered range: the 3rd mode of the beam and the (0,5) mode of the disc fall within this range.

The procedure for the evaluation of the effective normal stiffness consists in extracting the eigenvalues of the model as a function of k_n and comparing the split of the disc modes with the split coming from the model. Fig. 12 shows the results of this procedure. Five mode pairs of the disc ((0,3), (0,4), (05), (0,6), and (0,7)) are used: for each of them the frequency split in the FRF is measured and, for each considered mode, the corresponding value of the normal stiffness is evaluated from the output of the model, obtaining the average value $k_n = 5.2 \times 10^7$ N/m.

The mass of the pad m is evaluated by measuring the eigenvalue sensitivity to mass variations.

For a single degree of freedom system, characterized by a mass m and a stiffness k, it is:

$$\omega_a^2 = \frac{k}{m}, \quad \omega_b^2 = \frac{k}{m+\varepsilon} \Rightarrow m = \frac{\omega_b^2 \varepsilon}{\omega_a^2 - \omega_b^2}, \tag{23}$$

where ε is a small mass added to the pad, ω_a is the natural frequency of the pad and ω_b is its natural frequency when the mass ε is added.

Adding a mass $\varepsilon = 0.25$ g, the value $\omega_b = 10.030$ Hz is measured, which provides the result m = 6.3×10^{-2} kg.

The damping loss factor η, introduced in the model to take into account the hysteretic damping of the pad, (i.e. $k_p = k^*_p(1+j\eta)$ and $k_n = k^*_n(1+j\eta)$), is evaluated by the commercial software ART&MIS to be around 6%.

References

[1] H.R. Mills, Brake squeak, *Technical Report 9000 B, Institution of Automobile Engineers*, 1938.

[2] R.A.C. Fosberry, Z. Holubecki, Interim report on disc brake squeal, *Technical Report 1959/4, Motor Industry Research Association,* Warwickshire, England, 1959.

[3] R.A.C. Fosberry, Z. Holubecki, Disc brake squeal: its mechanism and suppression, *Technical Report 1961/1, Motor Industry Research Association,* Warwickshire, England, 1961.

[4] R.T. Spurr, A theory of brake squeal, *Proceedings of the Automobile Division, Institution of Mechanical Engineers* 1961–1962 (1) (1961) 33–52.

[5] S.W.E. Earles, G.B. Soar, Squeal noise in disc brakes, In: *Vibration and Noise in Motor Vehicles, Institution of Mechanical Engineers*, London, England, 1971, pp. 61–69, Paper number C 101/71.

[6] S.W.E. Earles, A mechanism of disc-brake squeal, *Technical Report 770181*, SAE, Warrendale, PA, 1977.

[7] R.P. Jarvis, B. Mills, Vibrations induced by friction, *Proceedings of the Institution of Mechanical Engineers* 178 (32) (1963) 847–857.

[8] M.R. North, Disc brake squeal, a theoretical model, *Technical Report 1972/5, Motor Industry Research Association*, Warwickshire, England, 1972.

[9] M.R. North, Disc brake squeal, In: *Braking of Road Vehicles, Automobile Division of the Institution of Mechanical Engineers*, Mechanical Engineering Publications Limited, London, England, 1976, pp., 169–176.

[10] J.E. Mottershead, Vibration- and friction-induced instability in disks, *Shock and Vibration Digest* 30 (1) (1998) 14–31.

[11] S.N. Chan, J.E. Mottershead, M.P. Cartmell, Parametric resonances at subcritical speeds in discs with rotating frictional loads, *Proceedings of the Institution of Mechanical Engineers Part C* 208 (C6) (1994) 417–425.

[12] H. Ouyang, J.E. Mottershead, M.P. Cartmell, M.I. Friswell, Friction-induced parametric resonances in discs: effect of a negative friction-velocity relationship, *Journal of Sound and Vibration* 209 (2) (1998) 251–264.

[13] H. Ouyang, J.E. Mottershead, D.J. Brookfield, S. James, M.P. Cartmell, A methodology for the determination of dynamic instabilities in a car disc brake, *International Journal of Vehicle Design, Special Issue on Brake Roughness, Noise, Vibration and Dynamics* 23 (3/4) (2000) 241–262.

[14] G.D. Liles, Analysis of disc brake squeal using finite element methods, *Technical Report 891150*, SAE, Warrendale, PA, SAE, 1989.

[15] A. Tuchinda, N.P. Hoffmann, D.J. Ewins, W. Keiper, Effect of Pin Finite Width on Instability of Pin-On-Disc Systems, *Proceedings of the International Modal Analysis Conference – IMAC*, Vol. 1, pp. 552–557, 2002.

[16] P. Blaschke, M. Tan, A. Wang, On the analysis of brake squeal propensity using nite elements, *Technical Report 2000-01-2765*, SAE, Warrendale, PA, 2000.

[17] N. hinrichs, M. Oestreich, K. Popp, On the modeling of friction oscillator, *Journal of Sound and Vibration* 216 (3) (1998) 435–459.

[18] R. Allgaier, L. Gaul, W. Keiper, K. Willnery, N. Hoffmann**,** A study on brake squeal using a beam on disc, *Proceedings of the International Modal Analysis Conference – IMAC*, Vol. 1, pp. 528–534, 2002.

[19] O. Giannini, A. Akay, F. Massi, Experimental analysis of brake squeal noise on a laboratory brake setup, *Journal of Sound and Vibration* 292 (1-2) (2006) 1–20.
[20] Akay, J. Wickert, Z. Xu, Investigation of mode lock-in and friction interface, *Final Report, Department of mechanical engineering*, Carnegie Mellon University 2000
[21] Tuchinda, A., Hoffmann, N. P., Ewins, D. J. and Keiper, W., Mode Lock-in Characteristics and Instability Study of the Pin-On-Disc System, *Proceedings of the International Modal Analysis Conference – IMAC*, Vol. 1, pp. 71–77,2001.
[22] R. Allgaier, Experimentelle und numerische untersuchungen zum bremsenquietschen, Ph.D. thesys, University of Stuttgart, reihe12 Nr481.
[23] Y. Denou, M. Nishiwaki, First order analysis of low frequency disk brake squeal, *Technical Report* 2001-01-3136, SAE, Warrendale, PA, 2001.